Renewable and Sustainable Energy Reviews 30 (2014) 479–489

Contents lists available at ScienceDirect

Renewable and Sustainable Energy Reviews

journal homepage: www.elsevier.com/locate/rser

High-resolution model-based wind atlas for Greece

V. Kotroni*, K. Lagouvardos, S. Lykoudis

Institute for Environmental Research, National Observatory of Athens, Lofos Koufou, P. Penteli, 15236 Athens, Greece

ARTICLE INFO

Article history:
Received 29 March 2013
Received in revised form
3 October 2013
Accepted 19 October 2013
Available online 15 November 2013

Keywords:
Wind atlas
Model simulations
Wind potential
Greece

ABSTRACT

In the frame of this paper a wind climatology has been built for Greece, based on high resolution model simulations performed for a typical year of wind conditions over the area. The methodology followed includes: (a) the development of a typical wind year, (b) the definition of a modeling strategy and the performance of the appropriate simulations, (c) the verification of the 10-m wind speed simulated by the model against observations, (d) the statistical analysis of the wind simulations for the construction of the wind atlas. The analysis is performed at 50 m and includes gridded wind speeds, the parameters of the respective Weibull distributions, and the potential power production. Finally a discussion on the effect of the topography height and slope on the wind distribution and consequently on the wind potential density is provided.

Contents

1. Introduction . . . 479
2. Brief review of model based wind atlases . . . 480
3. The typical wind year . . . 481
4. Model simulations of the wind flow . . . 482
 4.1. Modeling strategy . . . 482
 4.2. Verification of the model simulations . . . 482
5. Statistical analysis of the wind . . . 484
 5.1. Mean wind speed . . . 484
 5.2. Wind potential . . . 484
6. Concluding remarks . . . 486
Acknowledgments . . . 488
References . . . 488

1. Introduction

Wind energy offers significant potential for near- and long-term carbon emissions reduction. The wind power capacity installed by the end of 2009 was capable of meeting roughly 1.8% of the worldwide electricity demand, and that contribution could grow to in excess of 20% by 2050 if reducing greenhouse gas emissions was to be considered as a high priority goal and considerable efforts were made to address impediments to increased wind energy deployment [1]. During the last decade the wind energy market has expanded rapidly. From a cumulative capacity of 14 GW by the end of 1999, global installed wind power capacity increased 12-fold in 10 years to reach almost 160 GW by the end of 2009. Regionally, Europe continues to lead the market with 76 GW of cumulative installed wind power capacity by the end of 2009, representing 48% of the global total [2].

The Hellenic Government has set a target of 20% share of renewable energy in the gross final energy consumption by 2020. The contribution of renewable energy sources (RES) to the national energy balance in 2008 was approximately 7.8% of the gross final energy consumption and around 16.3% of the primary energy production. From the 1.64 Mtoe of primary energy produced from RES in 2008, 193 ktoe (~11.7%), have been produced by wind power plants [3]. The installed capacity of wind farms in Greece in

* Corresponding author. Tel.: +30 210 8109126; fax: +30 210 8103236.
E-mail address: kotroni@noa.gr (V. Kotroni).

1364-0321/$ - see front matter
http://dx.doi.org/10.1016/j.rser.2013.10.016

2011 was 1635.87 MW out of the 2511.60 MW of total installed capacity of renewable energy resources [4] while the installed capacity of wind power plants by 2020 is expected to exceed 7000 MW.

Based on the aforementioned information and taking into consideration the increase in the wind energy market, the identification of potential sites for wind farms is of high interest and therefore the need of construction of a wind atlas over Greece is considered to be of high priority. The complexity of the terrain of Greece arises from its orography but also from the land-water distribution and the large number of islands. Therefore the production of an accurate wind atlas is also a quite complex task. Indeed, a wind atlas for Greece has been produced in 2006 [5] and updated in 2008, based on the use of measured winds over the Greek territory and the application of a mass-consistent model. Results of this wind atlas are given at the official web page of the Greek Regulatory Authority for Energy (http://www.rae.gr/geo/).

Many wind atlases that have been recently produced for various countries have been based on the use of numerical weather prediction models (NWP) which are accompanied in some cases with the use of diagnostic downscaling models. A review of recent efforts in producing model based wind atlases, including the existing wind atlas for Greece, is given in Section 2 of this paper.

Thus, based on the international practice to use NWP models for the construction of wind atlases, the National Observatory of Athens took the initiative to build a wind climatology for Greece based on high resolution model simulations performed for a typical year of wind conditions over Greece. This effort is considered as complementary to the existing wind atlas that is based on the use of a mass-consistent model. The adopted methodology consists in defining a typical wind year over Greece that then is simulated using a mesoscale model for a domain covering Greece. In order to better represent the complex topography of Greece and the land-sea distribution a fine horizontal grid increment of 2 km $\times$ 2 km has been selected. The simulated wind fields have been verified against surface station observations in order to assess the model ability to reproduce the local wind flow. Finally the model simulated winds at various heights have been statistically analyzed for the construction of the wind atlas.

The rest of the paper is structured as follows. The next section presents a review of model based wind atlases presented in the literature, while in Section 3 the methodology adopted for the definition of the typical wind year over Greece is presented. Section 4 is devoted to the presentation of the modeling strategy and the verification of the model simulations, while Section 5 discusses the resulting wind fields that are used for the construction of the wind atlas. The last section of the paper is devoted to the concluding remarks of this work.

2. Brief review of model based wind atlases.

Many wind atlases that have been recently presented in the literature have been based on the use of either NWP models, or microscale models such as Computational Fluid Dynamics (CFD) models or mass-consistent type models, or a combination of mesoscale/microscale models. Indeed, the Swedish wind atlas has been produced based on the simulation of 192 samples selected to represent the meteorological conditions governing the wind climate of Sweden, using the CFD hydrostatic model of the Meteorological Institute Uppsala University (MIUU). The method used is applicable for mapping wind resources with a resolution of 0.5–10 km and the data needed are geostrophic wind, land and sea temperatures, topography, roughness and land-use. The simulations were made for 3 values of the geostrophic wind speed, for 16 wind direction sectors and for 4 representative months (January, April, July and October) to account for the seasonal variations in temperature. In addition, observations from six surface stations along with the National Center for Environmental Predictions (NCEP hereafter) reanalysis fields at the 850 hPa pressure level were used to weight the influence of the geographical variation of the geostrophic wind into the results regarding the modeled wind climate [6].

Mederos et al. [7] presented a methodology to construct an offshore wind atlas for Canary Islands based on observations and model simulations. The authors produced mean 10-m wind speeds from daily wind data provided by QuickSCAT satellite for a 4 year period (2003–2006) at a resolution of 20 km and from 6-h winds obtained from HIRLAM model for the period 2002–2006 at 9-km resolution. The mean model values have been corrected based on the satellite data by establishing maximum and minimum values at 115% and 85% of the calculated mean value and values outside these limits were corrected and restricted to them. The “corrected” mean wind field of HIRLAM was used to “correct” with the same methodology the mean wind field produced from 3-h winds from MM5 model for the period 2004–2006 at 3-km resolution. Finally the resulting mean wind speed and mean direction at 10 m height with 3 km resolution are corrected with data from 40 anemometer stations. The authors concluded that a great offshore wind power resource is available in the Canary Islands.

Gastón et al. [8] presented a wind resource map of Spain that was built using Eta/Skiron NWP model. The authors analyzed 365 simulations covering one year (2006) at a horizontal resolution of 0.1 $\times$ 0.1 deg. The presented wind atlas only focus on the statistical analysis of winds at 10-m. Following a similar methodology Costa et al. [9] developed a wind atlas for Portugal using model simulations with MM5 model for a whole year (1999) using four nested domains with 81, 27, 9 and 3 km grid resolution. For the model validation, observations from four surface meteorological stations were used. The results of the one year simulations were corrected with the mean deviation factor between the mean wind speed in 1999 and the long term mean wind speed recorded at 4 anemometric stations, in order to consider the intra annual variability of the wind. The analysis focuses at three height levels (10-m, 60-m and 80-m).

The wind atlas of Italy [10], first developed in 2002 and refined in 2006 is based on the use of the mass-consistent WINDS (Wind field Interpolation by Non-Divergent Schemes) flow model developed at the University of Genoa. The authors have calculated the frequency distribution of wind speed and direction at 5000 m above ground level, provided by the European Centre for Medium-range Weather Forecast (ECMWF) reanalyses fields for the period 1990–1999. 48 simulations (for 3 values of the wind speed and for 16 directions) have been produced, for a number of sub-areas, in order to cover the whole area of interest. The model was applied to obtain preliminary wind maps from geostrophic wind data, taking into account orography and terrain roughness. It should be noted that this methodology does not take into account local meteorological effects that are not related to the wind aloft (e.g. land and sea breezes). Every simulation has been weighted using the corresponding statistical frequency of the climatological wind aloft. Finally the simulated mean annual wind fields have been corrected through a “correction factor” obtained taking into account measured data from over 400 stations scattered all over Italy. The model was applied to a grid of about 1 $\times$ 1 km. The refined wind atlas comprises the whole Italian land surfaces as well as the offshore areas up to 40 km from the coastline.

Tammelin et al. [11] prepared the Finnish wind atlas by applying a series of models. The authors used initial and boundary conditions from the ERA-Interim data base and applied HIRLAM hydrostatic model at a resolution of 7.5 km over northern Europe

in order to provide initial and boundary conditions to the non-hydrostatic model AROME with 2.5 km horizontal resolution over Finland. The authors produced simulations for a period of 48 months in total (4 Januaries, 4 Februaries, etc.) that were selected as representative of the period 1989–2007. Moreover they have also simulated the windiest and the calmest months of the same period. The selection of the representative months was based on the fulfillment of the following criteria: the Weibull distribution of the wind speed should be as representative as possible for the selected period and in the 12 wind direction sections while also the distribution of wind directions should be also as representative as possible. In addition to the NWP models, the diagnostic downscaling method Wind Atlas Analysis and Application Programme (WAsP) [12] with 250 m resolution has been also applied only over the areas most favorable for wind power production. Further information on the Finnish wind atlas can be found at: http://www.tuuliatlas.fi/en/index.html.

Finally the Canadian Wind Atlas has been constructed using a three step procedure consisting of: (a) classifying the wind regimes such as to produce a climate state database based on NCEP reanalysis data, (b) producing simulations with MC2 mesoscale non-hydrostatic model at 5 km resolution, and (c) downscaling with a microscale modeling technique (MsMicro) which uses the wind energy statistics to determine wind patterns at microscale [13]. The method is presented in detail in [14] and has been recently used to produce a high resolution wind atlas for Thailand [15]. A detailed review of the methods for wind resource estimation can also be found in [16].

For Greece, the wind atlas produced in 2006 [5] and updated in 2008 has been based on the use of measured winds over the Greek territory and the use of a mass-consistent model (namely CRES-flowPot, see [17]). The methodology is based on the assumption that the wind flow at high altitudes is not influenced by the surface boundary layer, while close to the surface the combined effect of the topography and the boundary layer is sufficient to determine the wind speed and direction at any given point. The wind flow has been defined for 8 directions and normalized by the wind at the upper boundary. The normalized values of the study area have been then converted to actual wind speeds for each direction independently. Indeed, using time-averaging information (probability density function of the wind direction) that resulted from the measurements, wind speed has been calculated for each point as an average value. The characterization of the wind climatology over Greece has been based on the use of 200 measuring stations deployed over Greece for various periods by the Centre for Renewable Energy Sources (CRES), the Hellenic National Meteorological Service (HNMS) and the National Observatory of Athens (NOA). The available datasets included short-term (18 months) and long-term (10 years) measurements at various heights and periods. The datasets have been analyzed and correlated using the WindRose software tool developed at CRES (http://www.windrose.gr) [5]. The results on the latest version of this wind atlas are provided on a mesh with a horizontal resolution of 150 m and they are shown at the official web page of the Greek Regulatory Authority for Energy (http://www.rae.gr/geo/).

3. The typical wind year

The performance of wind turbines, much like solar systems, depends both on the long term-climatic-characteristics as well as the short term variations of weather conditions. Therefore, to predict the energy generated from such systems in the design stage, appropriate weather data is required. When the task at hand involves high resolution simulations the period that has to be simulated also needs to be carefully considered both in terms of representativity and in terms of efficiency/cost. In that respect running a multiyear simulation with a NWP model should provide adequately representative results otherwise it would be completely inefficient. A possible way around this would to be to run the simulation for a single year with typical/representative weather conditions. Apart from the long term this would also take into account any possible seasonal variability as well as the short term fluctuations.

Methodologies for generating weather data sets appropriate for this kind of studies, named Test Reference Years, Typical Meteorological Years (TMY) etc., have been in existence for many years, e.g. [18,19]. These data sets usually consist of 1 year of hourly data for the various meteorological parameters; temperature, humidity, solar radiation and wind are almost always included. These methodologies can be divided into two major categories: (a) those generating synthetic data sets with statistical properties reproducing those of the long-term dataset, (b) those using sub-periods from the actual data set – usually months – with statistical properties best resembling those of the long-term data for that sub-period [20–23].

The existing TMY data sets of this kind were mostly intended for building energy and solar system simulations, thus the relative importance of wind in the selection procedure has been small and therefore they are inappropriate for a study of wind power potential [24].

For that reason, and in order to support the objective of the current study, a typical year based only on the wind flow over Greece and the surrounding maritime areas has been defined. For the definition of the typical year, the ECMWF meteorological reanalysis fields of 10-m wind speed and direction for the 20-year period 1989–2008 have been used. This ECMWF-Interim database provides data with $\sim$80 km spatial resolution, at 6-h intervals. The selected area, for which the typical meteorological year was built, is bounded from 18 E to 30 E and from 34 N to 42 N.

The typical wind year consists of months selected from individual years, concatenated to form a complete year. As for the present application – the development of a wind-atlas – the parameters used from the ECMWF-Interim database are the 10-m wind speed and direction at 6 h intervals for the aforementioned period. The methodology used in order to define the typical months is based on that introduced by Hall et al. [18] and proposed in [21] using the Filkenstein-Schafer statistic [25]. Indeed, the cumulative distribution functions (CDFs) based on 160 wind bins (20 bins for the wind speed by 8 bins for the wind direction) have been calculated for each month, for each specific year of the 20 year period as well as for the entire 20 year period (long term CDF) for the same month. Then the wind CDF (speed and direction) for each month for each specific year is compared with the respective CDF of the long-term 20 years composite. From the 20 months, the one for which the sum of the absolute differences between the two CDFs is minimal, is selected for the typical wind year.

According to the aforementioned methodology the typical meteorological year constructed includes the monthly sequence given in Table 1.

Table 1
List of the 12 months and respective years that define the typical wind year.

Month	*Year*	*Month*	*Year*
January	1999	July	2008
February	1996	August	1997
March	2000	September	2008
April	1995	October	1994
May	1998	November	2007
June	2006	December	2003

4. Model simulations of the wind flow

4.1. Modeling strategy

As already presented in Section 3, model based wind atlases are based on the use of NWP models (such as HIRLAM, MC2, Eta, MM5, etc.) or microscale models or a combination of them. The microscale models are diagnostic models that are dedicated to the study of atmospheric processes that do not exceed a couple of kilometers and range from the simple versions (mass-consistent models, or more evolved linearized Navier–Stokes equation models, e.g. WAsP, WINDS, MsMicro) to the advanced and computationally demanding CFD models (e.g. MIUU) [16,26,27].

In the frame of this study the authors decided to use a NWP model for the construction of the wind atlas over Greece as the existing atlas has been based on the use of a mass-consistent model that is unable to include atmospheric parameters such the influence of atmospheric stability on the definition of the flow in the boundary layer, the development of local circulations (such as the sea breeze, katabatic winds, etc.) and the effect of Coriolis force. The advantage of the use of NWP model for the definition of the wind atlas is that the same model can be eventually used for the prediction of wind potential over an area (combined with a microscale model) creating thus a consistent strategy.

The model based wind atlas of this study is based on the use of the NWP model MM5. MM5 model is a non-hydrostatic, primitive equation model using terrain-following coordinates [28]. Several physical parameterization schemes are available in the model for the boundary layer, the radiative transfer, the microphysics and the cumulus convection. For both the operational chain of MM5 model at NOA but also for the model simulations for the wind atlas the combination of Kain and Fritsch [29] parameterization scheme with the highly efficient and simplified microphysical scheme proposed by [30] have been used as they provide the most skillful forecasts of accumulated precipitation over Greece [31,32]. Concerning the choice of the Planetary Boundary Layer (PBL) scheme, the scheme proposed by Hong and Pan [33] is used as this has proved to have a consistently good behavior in the region [34]. This model has been verified for its forecasting skill over Greece by Kotroni and Lagouvardos [35].

Two nested grids have been defined and used for the model simulations (Fig. 1). Grid 1 has 10-km horizontal grid increment (230×210 grid points), covering the major part of Southestern Europe, and the Balkans. Grid 2 has 2-km horizontal grid increment (431×436 grid points), covering the Greek territory and all the Greek islands and the adjacent water bodies. The horizontal extension of the defined grids is shown in Fig. 1a. In the vertical, forty unevenly spaced full sigma levels are selected.

For each day of each month of the typical wind year, four simulations are performed starting at 0000, 0600, 1200 and 1800 UTC with a 6-h duration for each simulation. All data from the 6-h simulations sequences are stored for further analysis at 1-h intervals from $t+1$ up to $t+6$ h of simulation. The ECMWF gridded analysis fields and 6-h interval, at 0.5-degree lat/lon horizontal grid increment, are used to initialize the model and to nudge the boundaries of Grid 1 during the simulation period.

4.2. Verification of the model simulations

In order to evaluate the model skill to provide accurate wind forecasts, a verification procedure is undertaken for each month of the defined typical year. The observational data include six weather stations distributed across Greece (Fig. 1b). All stations are located at airports and operated by the Hellenic National Meteorological Service for periods longer than the examined one (1989–2008). The wind speed value at the model grid point closest to the observational site has been used for the verification, while the four model points surrounding the observing station were also considered. This procedure permits to reduce the possibility of penalizing the model performance due to inconsistencies between model and actual topography.

The initial processing of the data, apart from consistency checking, included reduction of the model 10-m wind speed values, to the height of the observing stations, as well as binning of all data (modeled and observed) to 1 m s^{-1} intervals. This treatment, even though deviating from the 0.5 m s^{-1} recommended by the International Electrotechnical Commission (IEC) for wind turbines power performance measurements [36], was imposed by the fact that observed wind speeds were provided as integers. Furthermore, there are operational wind speed limits for power generation with wind turbines [37] that should be accounted for in the comparison. Thus, apart from the original, henceforth "complete" data set, we created a second dataset named "operational" by binning all data below or equal to a cut-in wind speed of 3 m s^{-1} into a single bin. The cut-off speed (25 m s^{-1}) was never reached in the analyzed dataset, so no specific treatment was necessary.

In order to select the model point that best simulates the wind data observed in each meteorological station, contingency tables for each pair of observed and modeled data sets were created and, for each contingency table, the Gamma-statistic of association as well as the associated standard error were calculated [38]. According to these statistics, wind speeds from any one of the 5 model points surrounding the observing station, represent the observed data equally well and in a statistically significant manner, either considering the complete or the operational data sets.

Wind direction, even though not of interest in this particular context was also checked using contingency tables of observed and modeled data binned according to 9 (per 45°+calms) or 5 (per 90°+calms) sectors. Only half of the 9-sector comparisons were statistically significant, whereas for 5-sectors only one station (Larissa) was not significant. However, as in the case of wind speed, there was no clearly discernible pattern as to which model points better represent the observations at each station.

Based on the above, the model point closest to the observing station was used for the model performance evaluation. Basic model evaluation statistics for the model point closest to each station, and for both the complete and the operational data sets, are presented in Table 2. The model, on average over the entire wind speed range (complete dataset), overestimates wind speeds at mainland stations (Aktion, Alexandroupoli and Larissa), while it slightly underestimates wind speed at the island station of Limnos. When the operational data set is considered (wind speeds less or equal to 3 m s^{-1} are removed) only slight overestimation remains at the mainland stations Alexandroupoli and Larissa, whereas wind speed is slightly underestimated at all other stations. The rest of the model performance statistics, also improve when we consider the operational data set instead of the original one, with a MAE around 2.2 m s^{-1}, and Pearson correlation coefficients, r, exceeding 0.4 except for Larissa and Aktion.

The typical point-to-point comparison presented above is useful in a general case, however it might not be the best choice in the specific context of our work. Since our goal is to provide credible information about the wind energy availability across Greece, it seems appropriate to focus on the comparison of the distributions describing the modeled and the observed wind speed data, rather than the data itself. The first logical step was to compare the empirical distributions of the modeled and the observed wind speeds. However empirical distributions are prone to reflecting the irregularities at the end points of the data, and in other places where the data is sparse, thus increasing the risk of a falsely negative ruling on the similarity of the modeled and the observed distributions. Furthermore, since our entire analysis

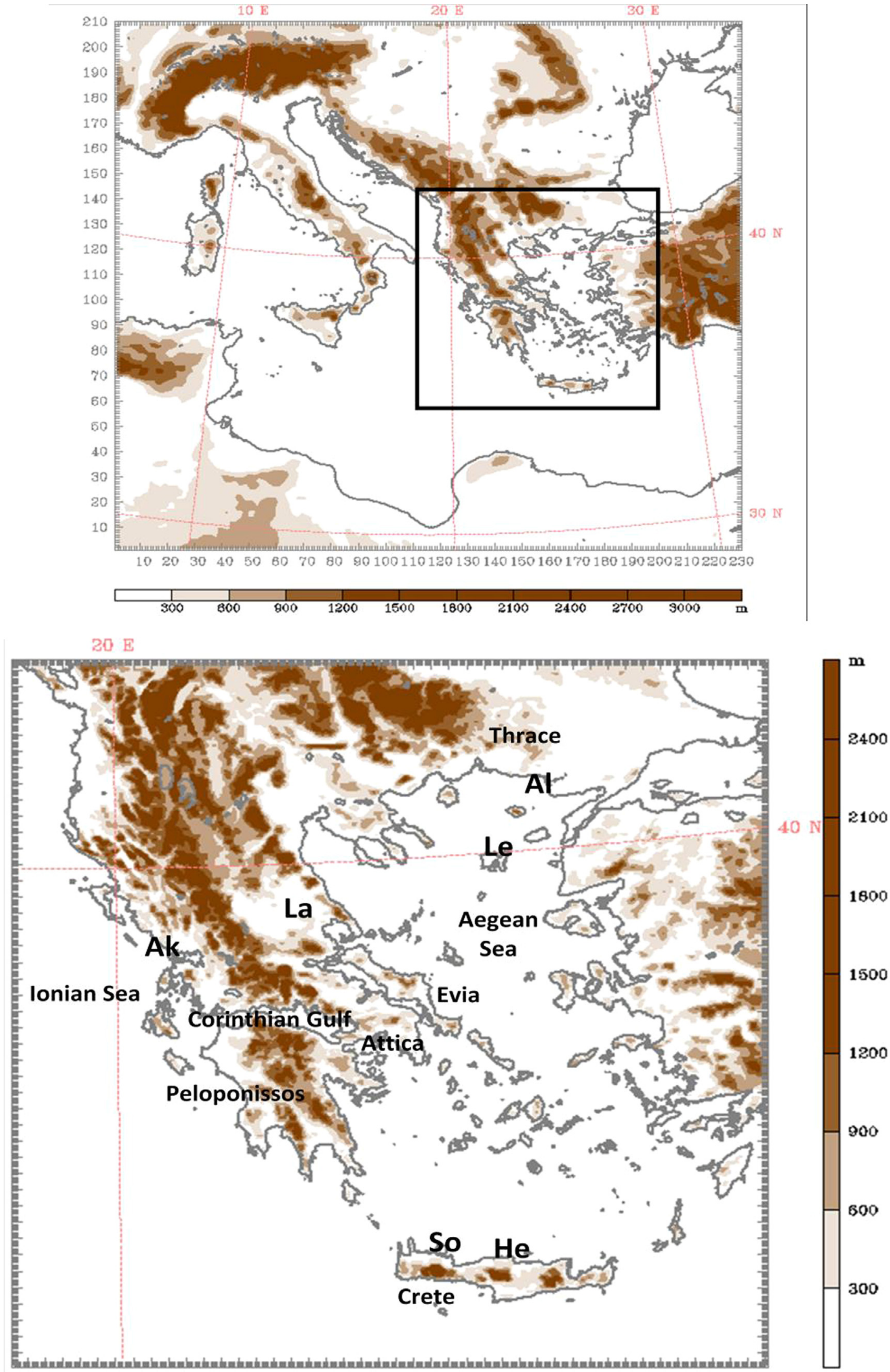


Fig. 1. (a) The two nested grids used for the simulations, (b) Inner model domain with the location of the surface stations used for the model verification: Alexandroupolis (A), Lemnos (L), Larissa (La), Aktion (Ak), Souda (S) and Heraklion (H). Model topography height (in m) is also shown.

Table 2
Model evaluation statistics: Pearson correlation coefficient (r), Mean Bias Error (MBE), Mean Absolute Error (MAE) and Root Mean Square Error (RMSE) for the model point closest to each station, for the complete (C) and the operational (O) datasets.

	r		MBE (m s^{-1})		MAE (m s^{-1})		RMSE (m s^{-1})	
	C	O	C	O	C	O	C	O
Alexandroupoli	0.49	0.47	1.4	0.4	2.4	2.2	3.0	2.8
Limnos	0.53	0.57	−0.7	−1.0	2.7	2.5	3.3	3.1
Larissa	0.18	0.15	3.0	0.5	3.4	2.1	4.0	2.8
Aktion	0.33	0.21	1.5	−0.1	2.7	2.2	3.3	2.8
Souda	0.41	0.43	0.2	−0.7	2.4	2.3	3.0	2.9
Heraklion	0.31	0.41	−0.2	−1.0	2.4	2.4	3.0	3.1

Table 3
Kolmogorov–Smirnov test, D statistic, the respective critical values for the 5% level of significance.

	D	
	C $D_{crit}=0.119$	O $D_{crit}=0.132$
Alexandroupoli	0.193	0.110
Limnos	0.104	0.100
Larissa	0.236	0.020
Aktion	0.077	0.039
Souda	0.067	0.067
Heraklion	0.063	0.063

would be based on the fitted Weibull distributions for the model grid points, we preferred to use those as the basis of the comparison. An initial comparison using the Pearson correlation coefficients, r, indicated very close agreement ($r > 0.95$ in all cases) between the CDF's of the distributions fitted to the observed and modeled wind speed. Moreover, the non-parametric Kolmogorov–Smirnov test for the equality of two probability distributions [39] was applied to the Weibull distributions fitted on the observed and the modeled data for each station and for both the complete and the operational data sets.

Table 3 presents the resulting D statistics of the Kolmogorov–Smirnov test, as well as the respective critical values for the 5% level of significance. Values of D less than the critical level suggest that at the 5% level of significance, there is not enough evidence to reject the hypothesis that the two samples follow the same distribution. For the original set, at Alexandroupoli and Larissa the Kolmogorov–Smirnov test suggests that the modeled wind speeds do not follow the same distribution as the observed ones. However when the operational data set is examined (wind speeds between 4 and 25 m s^{-1}) this discrepancy is removed and the Weibull distributions fitted on the modeled data are the same as those followed by the respective observed data.

5. Statistical analysis of the wind

5.1. Mean wind speed

The Wind Atlas includes monthly wind statistics for seven height levels: 50 m, 75 m, 100 m, 125 m, 150 m, 200 m and 400 m, and for a total of ~190.000 points, each representing an area of 2×2 km^2. The wind field has been analyzed at annual and monthly time scales, calculated from the hourly values. The area of the analysis covers Greece and the surrounding waters. In the following, the analysis focuses at the 50 m level winds. Fig. 2 presents the monthly average wind speed at 50 m for one representative month per season. Indeed, during January the mean wind speed is less than 3 m s^{-1} over the plains of continental Greece while over the medium and high altitudes the mean wind speed increases to more than 6 m s^{-1} (Fig. 2a). Among the continental areas, Northeastern Greece, Attica and the adjacent island Evia, southern Peloponissos and the southern part of Crete present the higher mean wind speeds. Among the maritime areas, the Aegean Sea is much windier than the Ionian Sea, with mean wind speeds ranging from 7 m s^{-1} up to more than 9 m s^{-1} locally. Increased wind speeds are also found in the entrance of the Corinthian Gulf, which is a narrow sea-level passage surrounded by a steep complex topography that consists of high mountains, elevated and sea-level gaps/straits. This is in agreement with the findings of Koletsis et al. [40] who found, in their wind climatology of the area that the most intense wind events occur during the winter season.

During spring, (Fig. 2b) the mean wind speed over Greece presents much less variability than in winter, with winds of the order of 3–4 m s^{-1} over the plains, increasing to 4–6 m s^{-1} with height, while over the maritime areas the prevailing wind are of the order of 5 m s^{-1}.

During summer (Fig. 2c), while over land the mean wind speed pattern is quite similar to that of spring, over Attica, Crete and the maritime areas and the islands of the Aegean sea the wind speed is considerably increased. Indeed, during summer northern sector winds are blowing over the Aegean Sea, the Etesian winds, which are mainly north-easterly in the northern Aegean, northerly in the central and southern Aegean and tend to become north-westerly near the southwestern Turkish coasts. The air masses regularly originate from the region of southern Russia and the Caspian Sea and they are dry and relatively cool, contributing to the decrease of surface temperature and the moderation of summer heat and discomfort [41,42]. The sustained wind speed associated with the Etesians often attain near-surface values exceeding 15 m s^{-1} [42]. As shown in Fig. 2c, the mean wind speed at 50-m, over the Aegean, increases to 7–8 m s^{-1} and locally reaches more than 11 m s^{-1}.

Autumn is the rainiest season in Greece which is affected by the passage of low pressure systems associated with southerly winds [43]. The mean wind speed distribution at 50-m is relatively close to that during winter with the windiest areas found over the Aegean, Attica, Evia, the Corinthian Gulf area and Thrace in northeastern Greece (Fig. 2d).

5.2. Wind potential

The model simulated winds at hourly intervals at 50-m height have been used in order to determine the wind potential. If $f(\nu)$ is the probability density function (PDF) of wind speed ν, the wind potential P can be expressed as:.

$$P(\nu)=\frac{1}{2}\rho\int_0^{\infty}\nu^3 f(\nu)d\nu \tag{1}$$

where ρ is the air density. This integral can be evaluated over a range of wind speeds and in the frame of this study it has been evaluated for the range of operation of wind turbines that usually ranges from a cut-in speed of 4 m s^{-1} up to the cut-off speed of 25 m s^{-1} with a step of 0.2 m s^{-1}.

The PDF of wind speed is important in numerous wind energy applications. [44] presented an extensive review of the available methods for its estimation. Among a variety of PDFs, the two parameter Weibull probability density function is the most widely used and accepted in the specialised literature on wind energy and other renewable energy sources [45]. Indeed, the wind speed probability density function is given by

$$f(\nu)=\frac{k}{c}\cdot\left(\frac{\nu}{c}\right)^{k-1}\exp\left[-\left(\frac{\nu}{c}\right)^{k}\right] \tag{2}$$

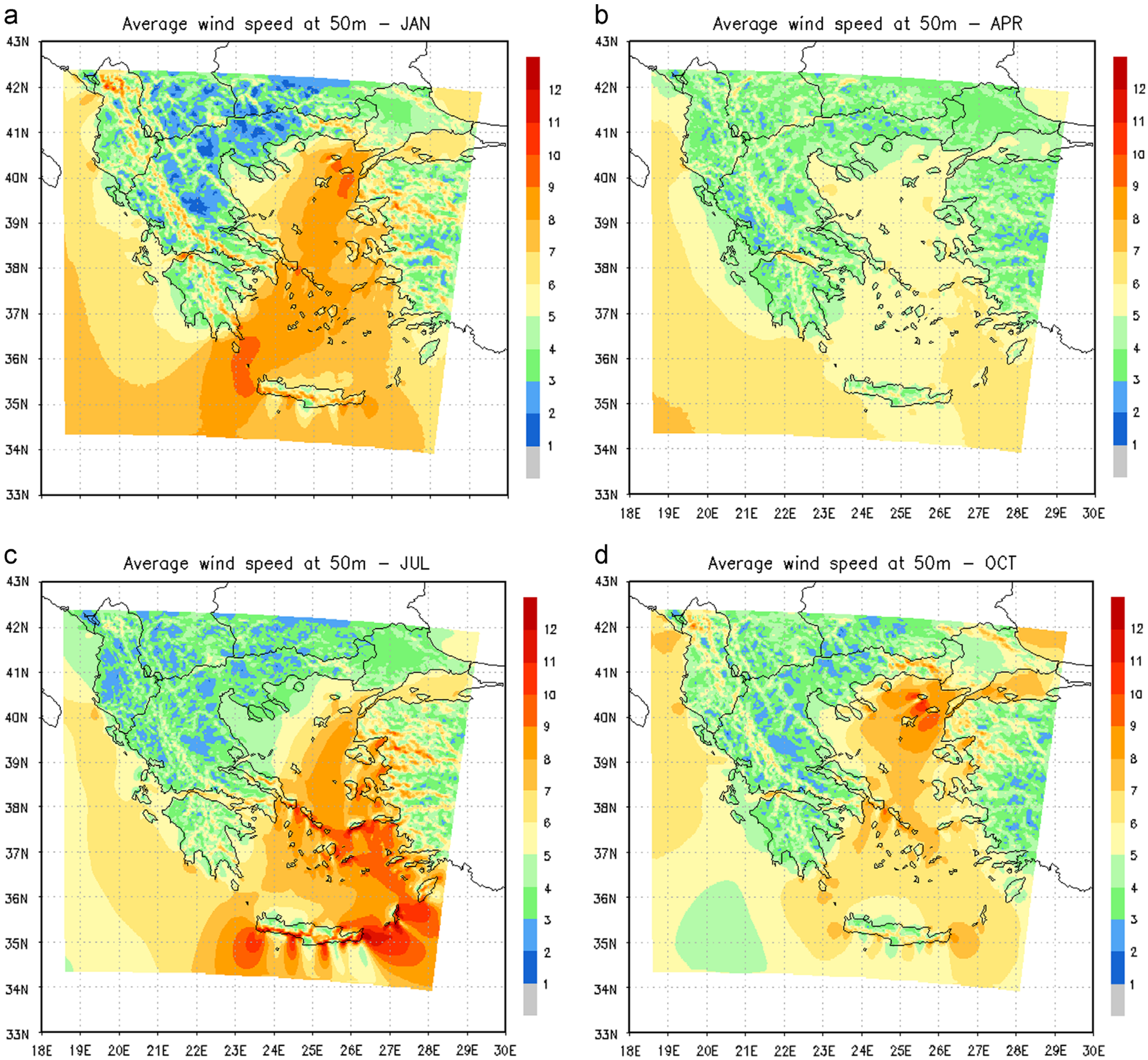


Fig. 2. Monthly mean wind speed (in m s^{-1}) at 50-m for (a) January, (b) April, (c) July and (d) October.

where c (in m s^{-1}) is the Weibull scale parameter and k (*dimensionless*) is the Weibull shape parameter that characterizes the asymmetry of the probability function. There are various methods to determine these two parameters.

In the frame of the present work, for the estimation of the two parameters the least square method has been used (see [44]). Indeed, the shape parameter k can be estimated through the following equation:

$$k=\left\{N\sum_{i=1}^{N}Y_iX_i-\left(\sum_{i=1}^{N}X_i\right)\left(\sum_{i=1}^{N}Y_i\right)\right\}\cdot\left\{N\sum_{i=1}^{N}X_i^2-\left(\sum_{i=1}^{N}X_i\right)^2\right\}^{-1} \quad (3)$$

where

$Y_i=ln\{-ln(1-P_i)\}$ and $X_i=ln(v_{max,i})$

and P_i are the components of the vector P which contains the cumulative relative frequencies of the N intervals in which the n wind speeds of the sample have been classified, $v_{max,i}$ are the maximum wind speed values within each of the N intervals. The scale parameter c is estimated from the following equation:

$$c=\exp\left[-\frac{b}{k}\right] \quad (4)$$

where b is estimated following:

$$b=\left\{\sum_{i=1}^{N}Y_i\sum_{i=1}^{N}X_i^2-\left(\sum_{i=1}^{N}X_i\right)\left(\sum_{i=1}^{N}X_i\cdot Y_i\right)\right\}\left\{N\sum_{i=1}^{N}X_i^2-\left(\sum_{i=1}^{N}X_i\right)^2\right\}^{-1} \quad (5)$$

Based on the above, once the wind potential is estimated a classification was made following [46]. Indeed, six classes of wind potential have been used as presented in Table 4.

Fig. 3 presents the mean yearly wind potential at 50-m that has been evaluated from a cut-in speed of 4 m s^{-1} to the cut-off speed of 25 m s^{-1} with a step of 0.2 m s^{-1} based on Eq. (1). It is clear

Table 4
Classification of wind potential density (adopted from the Texas State Energy Conservation Office).

Wind Power Class	Wind potential density ($W m^{-2}$)	Commercial viability
1	0–200	Very poor
2	200–300	Poor
3	300–400	Marginal
4	400–500	Good
5	500–600	Very good
6	> 600	Excellent

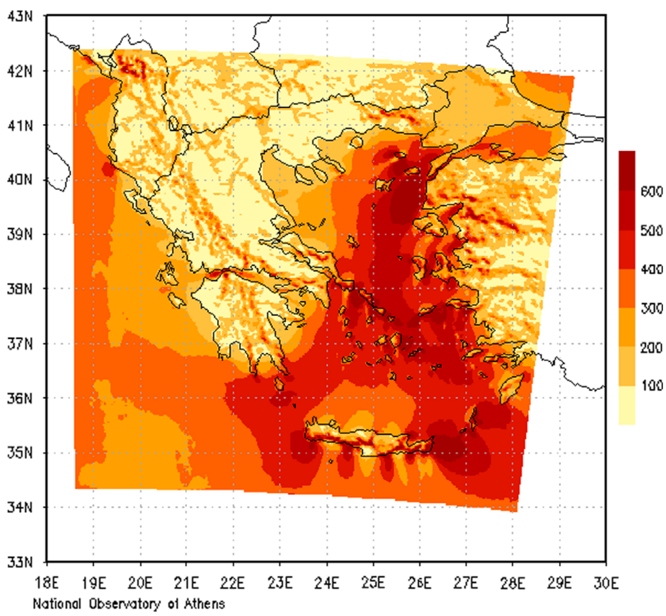


Fig. 3. Wind potential (in $W m^{-2}$) at 50-m.

that in the largest part of the Aegean sea the wind potential is larger than 500 $W m^{-2}$, reaching locally 700 $W m^{-2}$. Over the Ionian the wind potential is of the order of ~300 $W m^{-2}$. Locally the wind potential exceeds 400 $W m^{-2}$ over the mountain ranges as well as over the Corinthian Gulf, Thrace, Attica and Evia, southeastern Peloponnisos and Crete. Accordingly these areas are characterized by wind power class 3 or higher as depicted in Fig. 4. A zoom-in over the areas with the highest wind classes, namely Crete (Fig. 5a), and Attica and Evia (Fig. 5b) is given. It is evident that eastern Crete has a higher class wind power that locally is excellent (class 6), while southern Crete presents a better wind power class compared to the northern areas. This is related to the complex topography of Crete island that produces gap winds and acceleration of the wind flow over southern Crete [47,48]. The wind power class exceeds 5 over a large part of Southern Evia island, while offshore southern Evia the wind power class rates as excellent.

With the aim to investigate the effect of the topography height and slope on the wind distribution and consequently on the wind potential density, the cumulative frequency of wind power class for 7 classes of topography height and 5 classes of slope have been calculated. Namely, the selected topography bins are: < 200, 200–400, 400–600, 600–800, 800–1000, 1000–1500, > 1500 m) while the slope bins are: 0, 0.1–2, 2–5, 5–10, > 10). At this point it should be noted that the topography heights used are those used by the model at the 2 km × 2 km grid increment and thus they are smoothed compared to the actual topography heights. Moreover the sea points have been analyzed separately. The analysis (Table 5) shows that:

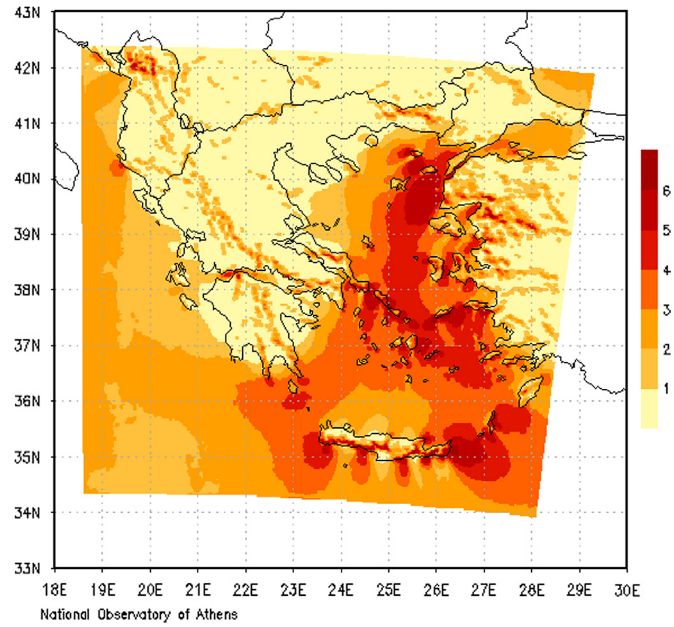


Fig. 4. Wind power class at 50-m.

- Almost 80–85% of all the land points with topography heights up to 1500 m are characterized by a wind power class of 1 (< 200 $W m^{-2}$) while the percentages of class 2 range from 8–13%, for class 3 range from 2.9–4.5% and only about 0.8% of the land grid points are characterized by a wind power class of 6.
- Grid points with heights above 1500 m present a higher wind potential density. Indeed ~60% of the points of this height bin are characterized by a wind power class of 1, while the percentages for classes 2 and 3 are 30% and 6%, respectively.
- The dependence of the wind potential density on the slope is more evident. The grid points of 0 slope are characterized by very poor wind potential density at a percentage of ~90%, 6% are classified to the class 2, ~2% to class 3 and only 1% of the points are classified in class 4 or higher. The grid points with slope up to 5%, present a better commercial viability. About 11–15% of them are in class 2, and almost 6% in class 3. Finally for the grid points with slopes larger than 5% the wind potential density distribution is even better. Indeed ~15% of the grid points are characterized by class 2 wind power, ~6% by class 3 and ~6% of the points are characterized by a wind class category of 4 or better.
- Analysis of the sea points showed that the offshore wind potential over the Greek seas is quite important as almost 70% of the marine grid points are characterized by a wind class of 3 or better, while ~34% of the grid points are classified in the wind power class of 4 or better.

6. Concluding remarks

In the frame of the present paper a Wind Atlas over Greece has been developed based on simulations performed with the numerical weather prediction model MM5 that has been actively utilized at the National Observatory of Athens since 2000. The atlas contains 12 months of weather model simulations where the winds and other variables are calculated for grid boxes 2 × 2 km^2 in size.

The methodology used in order to select typical months to form a typical wind year was based on the Filkenstein-Schafer statistical method [25] and it is described with details in Section 2. The typical wind year was simulated by MM5 in 6-h sequences,

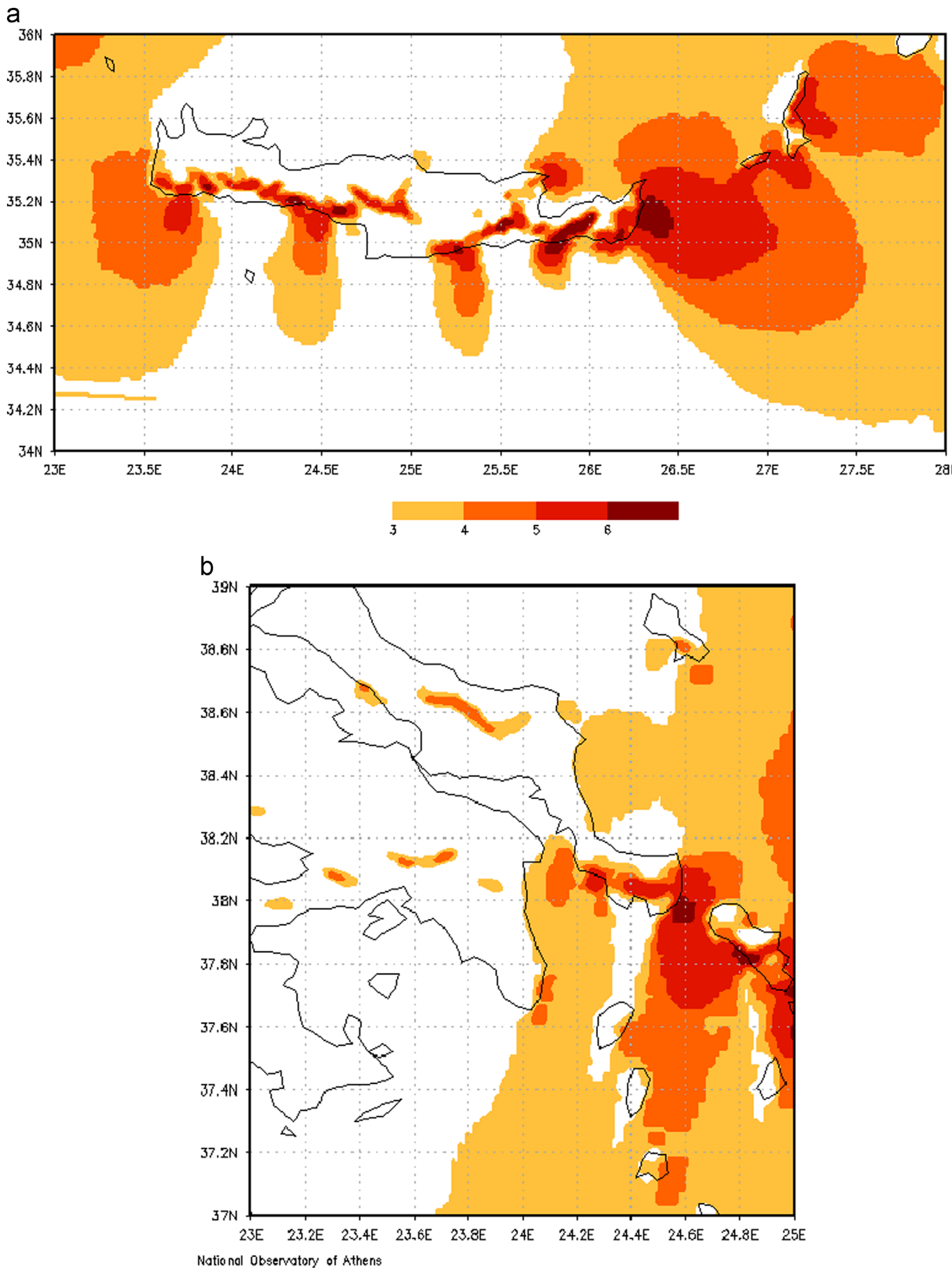


Fig. 5. Wind power class at 50-m. Zoom in Fig. 4 for (a) Crete island, (b) Attica and Evia areas. Only areas with class 3 or higher are shown.

storing the atmospheric state at 1-h intervals from $t+1$ up to $t+6$ h of simulation. The initial state of each 6-h sub-period and the required boundary conditions were provided by the European Centre for Medium-Range Weather Forecasts (ECMWF) analysis. The results of the model simulations have been verified against a number of surface meteorological stations while also annually and monthly statistics at various heights are produced over Greece and the surrounding maritime area.

The analysis showed that among the continental areas, North-eastern Greece, Attica and the adjacent island Evia, southern Peloponissos and the southern part of Crete present the higher mean wind speeds, while over the maritime areas, the Aegean Sea is much windier than the Ionian Sea. As for the seasonal variability of the mean wind speed, it was evident that during summer the wind speed is considerably increased over Attica, Crete and the surrounding maritime areas and the islands of the Aegean sea.

Table 5
Distribution of wind power classes (in %), in the studied domain according to 5 slope and 7 terrain height categories, as well as for the sea points.

		Wind power class					
		1	2	3	4	5	6
Slope	0	90.9	5.9	2.2	1.0	0.0	0.0
	0.1–2	80.7	11.9	4.3	2.0	0.7	0.4
	2–5	78.6	11.8	5.5	2.3	1.1	0.7
	5–10	72.8	15.1	5.8	3.2	1.4	1.7
	> 10	73.6	13.9	6.1	2.9	1.3	2.2
Terrain Height	< 200	85.7	10.0	3.2	0.8	0.2	0.1
	200–400	81.3	11.2	4.5	1.8	0.7	0.6
	400–600	80.4	11.1	4.5	2.4	0.9	0.8
	600–800	83.8	8.2	3.7	2.3	1.1	0.8
	800–1000	85.2	8.4	2.9	1.8	1.0	0.8
	1000–1500	80.9	12.9	4.0	1.3	0.4	0.6
	> 1500	62.1	29.2	5.9	1.3	0.6	0.9
	SEA	8.3	22.3	35.8	21.6	9.3	2.7

Moreover, in the largest part of the Aegean sea the wind potential is larger than 500 W m^{-2}, reaching locally 700 W m^{-2}. Over the Ionian the wind potential is of the order of ~300 W m^{-2}. Locally the wind potential exceeds 400 W m^{-2} over the mountain ranges as well as over the Corinthian Gulf, Thrace, Attica and Evia, southeastern Peloponnisos and Crete. These latter areas are characterized by wind power class 3 or higher.

Finally the investigation of the effect of the topography height and slope on the wind distribution and consequently on the wind potential density showed that the latter is more dependent on the slope than on the topography height. The analysis of the sea points showed that the offshore wind potential over the Greek maritime areas is quite important as almost 70% of the marine grid points are characterized by a wind class of 3 or better.

At this point it should be mentioned that for wind resource estimation and siting a detailed description of the terrain, namely the surface roughness, orography and obstacles, is required. In that case the Weibull distributions calculated over Greece could be used as input to a microscale model such as WaSP [12,49] together with detailed description of the terrain topography in order to estimate local wind climate for wind energy applications. Thus, it is in the authors plans to build a web-based interface that will make available the current wind atlas results for use for siting purposes.

Acknowledgments

The Hellenic National Meteorological Service is kindly acknowledged for the surface station data used for the model verification. The authors are also grateful to ECMWF for providing ERA-Interim reanalysis data used for the present study.

References

[1] Wiser R, Yang Z, Hand M, Hohmeyer O, Infield D, Jensen PH, et al. Wind energy. In: Edenhofer O, Pichs-Madruga R, Sokona Y, Seyboth K, Matschoss P, Kadner S, Zwickel T, Eickemeier P, Hansen G, Schlomer S, von Stechow C, editors. IPCC special report on renewable energy sources and climate change mitigation. Cambridge, United Kingdom and New York, NY, USA: Cambridge University Press; 2011.
[2] GWEC. Global wind 2009 report. Brussels, Belgium: Global Wind Energy Council (GWEC); 2010. 4 pp.
[3] Hellenic Ministry of Environment energy and climate change. National Renewable Energy Action Plan in the scope of directive 2009/28/EC; 2010.
[4] Papastamatiou P. Renewable Energy Sources in Greece within the crisis environment. In: Proceedings of the 4th InnoForum workshop on green economy: innovation & intellectual property rights. Athens Information Technology; 25 May 2012.
[5] Foussekis D, Chaviaropoulos PK, Vionis P, Karga I, Papadopoulos P, Kokkalidis F. Assessment of the long-term Greek wind atlas. In: Proceedings of the European Wind Energy Conference and Exhibition, Athens, Greece; 2006.
[6] Bergström H, Söderberg S. Wind mapping in Sweden—summary of results and methods used. Elforsk Rapp. 2008;09:04.
[7] Mederos, Martın AC, Medina Padron JF, Feijoo Lorenzo AE. An offshore wind atlas for the Canary Islands. Renew Sustain Energy Rev 2011;15:612–20.
[8] Gastón M, Pascal E, Frias L, Marti I.Wind resources map of Spain at mesoscale. Methodology and validation. In: Proceedings of European wind energy conference 2008, Brussels, Belgium; 2008.
[9] Costa P, Miranda P, Estanqueiro A. Development and validation of the Portuguese Wind Atlas. In: Proceedings of the European wind energy conference, Athens, Greece; 2006.
[10] Casale C, Lembo E, Serri L, Viani S. Italy's Wind Atlas: offshore resource assessment through on-the-spot measurements. Wind Eng 2010;34:17–28.
[11] Tammelin B, Vihma T, Atlaskin E, Badger J, Fortelius C, Gregow H, et al. Production of the Finnish Wind Atlas. Wind Energy 2011. http://dx.doi.org/10.1002/we.517.
[12] WAS. User's Guide, vol. 2. Risù-I-666(v. 2)(EN), Roskilde: Riso National Laboratory.
[13] Canadian Wind Energy Atlas at 5 km. EOLE Wind Energy Project. Available from: ⟨http://www.windatlas.ca⟩; 2005.
[14] Gasset N, Landry M, Gagnon Y. A comparison of wind flow models for wind resource assessment in wind energy applications. Energies 2012;2012 (5):4288–322.
[15] Waewsak J, Landry M, Gagnon Y. High resolution wind atlas for Nakhon Si Thammarat and Songkhla provinces Thailand. Renew. Energy 2013;53 (2013):101–10.
[16] Landberg L, Myllerup L, Rathmann O, Petersen EL, Jørgensen BH, Badger J, et al. Wind resource estimation—an overview. Wind Energy 2003;6:261–71.
[17] Chaviaropoulos P, Papadopoulos K, Kokkalidis F, Glinou G. Wind Climate in Greece. In: Proceedings of the EWEC, Madrid, Spain; 16–19 June 2003.
[18] Hall I, Prairie R, Anderson H, Boes E. Generation of typical meteorological years for 26 SOLMET stations. SAND78-1601. Albuquerque, NM: Sandia National Laboratories; 1978.
[19] Lund H, Eidorff S. Selection methods for the production of test reference years. Appendix D. Contract 284-77 ES DK. Final report. EUR 7306 EN; 1980.
[20] Argiriou A, Lykoudis S, Kontoyiannidis S, Balaras CA, Asimakopoulos D, Petrakis M, et al. Comparison of methodologies for TMY generation using 20 years data for Athens, Greece. Sol Energy 1999;66:33–45.
[21] ISO. ISO 15927-4. Hygrothermal performance of buildings—calculation and presentation of climatic data—part 4: hourly data for assessing the annual energy use for heating and cooling; 2005.
[22] Lhendup T, Lhundup S. Comparison of methodologies for generating a typical meteorological year (TMY). Energy Sustain Dev. 2007;11:5–10.
[23] Skeiker K. Comparison of methodologies for TMY generation using 10 years data for Damascus Syria. Energy Convers Manag 2007;48:2090–102.
[24] Yang HX, Lu L, Burnett J. Weather data and probability analysis of hybrid photovoltaic–wind power generation systems in Hong Kong. Renew Energy 2003;28:1813–24.
[25] Filkenstein JM, Schafer RE. Improved goodness of fit tests. Biometrica 1971;58:641–5.
[26] Petersen EL, Mortensen NG, Landberg L, Højstrup J, Frank HP. Wind power meteorology. Part II: Sitting and models. Wind Energy 1998;1:55–72.
[27] Ayotte K. Computational modelling for wind energy assessment. J. Wind Eng. Ind Aerodyn 2008;96:1571–90.
[28] Dudhia J. A non-hydrostatic version of the Penn State/NCAR nesoscale model: validation tests and simulation of an Atlantic cyclone and cold front. Mon Weather Rev 1993;121:1493–513.
[29] Kain JS, Fritsch JM. Convective parameterization for mesoscale models: the Kain–Fritsch scheme. The representation of Cumulus in numerical models. Meteor. Monogr., No 46, Amer Met, Soc; 1993. p. 165–177.
[30] Schultz P. An explicit cloud physics parameterization for operational numerical weather prediction. Mon Weather Rev 1995;123:3331–43.
[31] Kotroni V, Lagouvardos K. Precipitation forecast skill of different convective parameterization and microphysical schemes: application for the cold season over Greece. Geophys Res Lett 2001;108:1977–80.
[32] Mazarakis N, Kotroni V, Lagouvardos K, Argiriou AA. The sensitivity of numerical forecasts to convective parameterization during the warm period and the use of lighting data as an indicator for convective occurrence. Atmos Res 2009;94(4):704–14.
[33] Hong S-Y, Pan H-L. Nonlocal boundary layer vertical diffusion in a medium-range forecast model. Mon Weather Rev 1996;124:2322–39.
[34] Akylas E, Kotroni V, Lagouvardos K. Sensitivity of high resolution operational weather forecasts to the choice of the planetary boundary layer scheme. Atmos Res 2007;84:49–57.
[35] Kotroni V, Lagouvardos K. Evaluation of MM5 high-resolution real-time forecasts over the urban area of Athens, Greece. J Appl Meteorol 2004;43:1666–78.
[36] IEC, 2005: 61400-12-1 wind turbines: power performance measurements of electricity producing wind turbines.
[37] EEA. Europe's onshore and offshore wind energy potential. Technical report. No 6/2009; 2009.
[38] Goodman LA, Kruskal WH. Measures of association for cross classifications. J Am Stat Assoc 1954;49(268):732–64.
[39] Sprent P. Applied nonparametric statistical methods. 2nd ed. Chapman and Hall, London; 1993.
[40] Koletsis I, Kotroni V, Lagouvardos K. A model-based study of the wind regime over Corinthian Gulf in Greece. NHESS 2013 under review.

[41] Metaxas D, Bartzokas A. Pressure covariability over the Atlantic, Europe and N. Africa. Application: centers of action for temperature, winter precipitation and summer winds in Athens, Greece. Theor. Appl. Climatol. 1994;49:9–18.
[42] Kotroni V, Lagouvardos K, Lalas D. The effect of Crete island on the Etesian winds over the Aegean Sea. Q. J. R. Meteorol Soc 2001;127:1917–38.
[43] Lolis CJ, Bartzokas A, Lagouvardos K, Metaxas DA. Intra-annual variation of atmospheric static stability in the Mediterranean region: a 60-year climatology. Theor Appl Climatol 2012;110:245–61.
[44] Carta JA, Ramirez P, Velazquez S. A review of wind speed probability distributions used in wind energy analysis: case studies in the Canary Islands. Renew Sustain Energy Rev 2009;13:933–55.
[45] JV Seguro, Lambert TW. Modern estimation of the parameters of the Weibull wind speed distribution for wind energy analysis. J Wind Eng Ind Aerodyn 2000;85(1):75–84.
[46] Texas State Energy Conservation Office. Texas renewable energy resources. Available from: 〈http://www.infinitepower.org/reswind.htm〉; 2011.
[47] Koletsis I, Lagouvardos K, Kotroni V, Bartzokas A. The interaction of northern wind flow with the complex topography of Crete Island – Part I: observational study. Nat Hazards Earth Syst Sci 2009;9:1845–55.
[48] Koletsis I, Lagouvardos K, Kotroni V, Bartzokas A. The interaction of northern wind flow with the complex topography of Crete Island – Part II: numerical study. Nat Hazards Earth Syst Sci 2010;10:1115–27.
[49] Mortensen NG, Landberg L, Troen I, Petersen EL. Wind Atlas Anal Appl Progr 1993.